Hydrogeological, Hydrogeochemical and Isotope Geochemical Features of Thermal Waters in Simav and Environs

Olayinka A. BELLO[1], Nevzat OZGUR[2] and Tugba A CALISKAN[3]

1. Lagos, Nigeria.

2. Suleyman Demirel University, Department of Geological Engineering, Isparta, 32260, Turkey

3. Marmara Arastirma Merkezi, Center for Clean Production, Gebze-Kocaeli, Turkey.

[1] yinkabellong@gmail.com, [2] nevzatozgur@sdu.edu.tr, [3] tubacaliskan13@gmail.com

Keywords: Simav, Geothermal, Geothermometers, Hydrogeology, Hydrogeochemistry.

ABSTRACT

Simav geothermal field, one of Turkey's most important fields, is located in Kütahya's Simav graben system of western Anatolia. This is on the eastern part of the graben and approximately 4 km north of Simav town and on the NE edge of the Simav plain, which is separated from the mountain by a high and steep escarpment. The plain covers an area of about 70 km^2 and is at an altitude of about 780 m asl and lies on latitude 39^0 5' 23" N and longitude 28^0 58' 46" E.

The thermal waters of Simav can be classified as Na-HCO$_3$-SO4 type water with the dominant cations in increasing order of Na+K>Ca>Mg while the anions are HCO$_3$>SO$_4$>Cl. The Cl-SO$_4$-HCO$_3$ ternary diagram shows that the waters are peripheral/immature and more likely related to groundwater heated by steam from deeper reservoirs. Quartz, aragonite, calcite and chalcedony are oversaturated at discharge temperatures while at a recomputed temperature according to the reservoir composition, only quartz, dolomite and chalcedony are oversaturated. The silica geothermometer shows reservoir temperatures between 83 - 182^0C. The Na-K-Ca-Mg correction cation geothermometer gave reservoir temperatures close to the measured reservoir temperature on site in Eynal which is between 148 and 163^0C.

The waters plot along the meteoric trend line suggesting the source from local meteoric water and are rich in 18O. This situation points to the existence of fluid-interaction in the system and/or boiling due to the high temperature in the reservoir.

1. INTRODUCTION

Owing to the unsustainability of conventional fossil fuel, many countries are shifting focus and attention to alternative and renewable energies. Renewable energy is sustainable because the resources are used in a manner that provides ongoing energy to meet the needs of the current population, without compromising conditions for future generations. Geothermal energy is one of the many renewables available.

Geothermal fields are found throughout the world in a range of geological settings, and are increasingly being developed as an energy source. Each of the different types of geothermal system has distinct characteristics which are reflected in the chemistry of the geothermal fluids and their potential applications. However, they all have in common a heat source at a few kilometers depth, and it is this which sets water, present in the upper sections of the Earth's crust into convection (Nicholson, 1993).

Simav geothermal field, one of Turkey's most important fields, is located in Kütahya's Simav graben system of western Anatolia. This is on the eastern part of the graben and approximately 4 km north of Simav town and on the NE edge of the Simav plain, which is separated from the mountain by a high and steep escarpment. The plain covers an area of about 70 km^2 and is at an altitude of about 780 m asl and lies on latitude 39^0 5' 23" N and longitude 28^0 58' 46" E. The thermal water produced from this field is used for heating of the residential houses in the city (about 7000) while there is an ongoing effort in utilizing it for power generation.

The Purpose of this study is to understand the formation and development history of the thermal waters by hydrogeological, hydrogeochemical and isotope geochemical methods and to determine the water types in the geothermal area.

2. GEOTECTONIC LOCATION/GEOLOGICAL SETTINGS OF THE STUDY AREA

Turkey is located in the eastern Mediterranean segment on the Alpine–Himalayan earthquake belt and is frequently exposed to destructive earthquakes. There are seven major tectonic provinces in Turkey: the North Anatolian Fault (NAF), the Northeast Anatolian Fault (NEAF), the East Anatolian Contractional Province (EAF), the Aegean Graben System, the Cyprus–Hellenic Arc, the Central Anatolian Province, and the Black Sea region (Sengor et al., 1985). The tectonics of Turkey is greatly influenced by the movements of the Arabian, Eurasian, and African plates. Simav district is located within a collapsed basin (elevation 800 m) known as the Simav Graben in Western Anatolian province (Figure 1). Simav Mountain extends east–west and is located in the south of

Simav. The most important tectonic feature of the study area is Simav Fault, an active right strike-slip fault extending approximately 205km length in a general NW–SE direction (Konak, 1982; Saroglu et al., 1987, 1992).
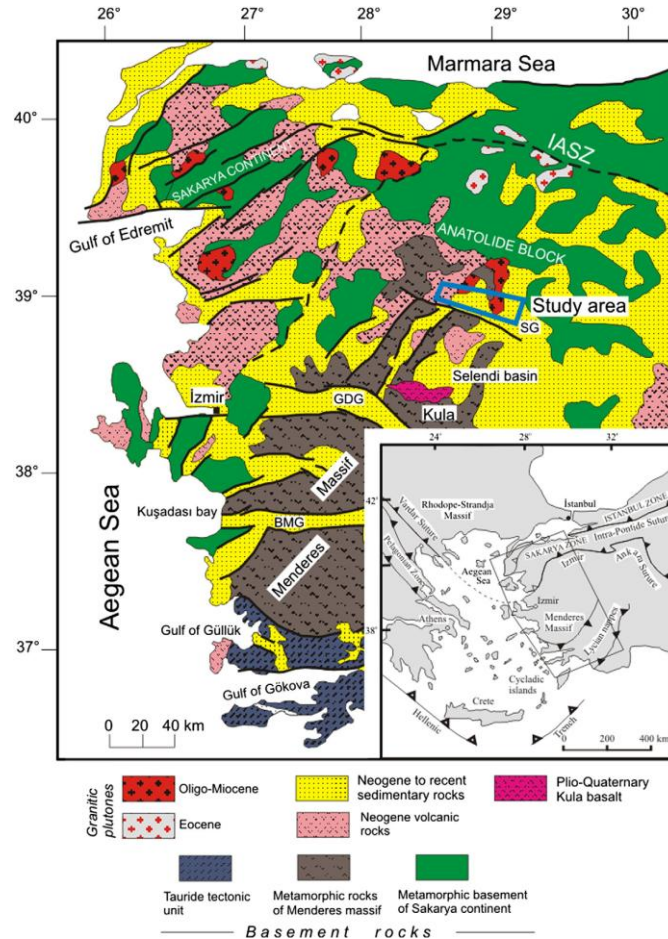

Figure 1: Main tectonics and geological units of western Anatolia. IASZ: İzmir-Ankara Suture Zone, SG: Simav graben, GDG: Gediz graben, BMG: Büyük Menderes graben (Yılmaz, 2000)

2.1 Geology

The Simav geothermal field is located in the eastern part of Simav graben, approximately 4km north of Simav town and on the NE edge of the Simav plain, which is separated from the mountain by a high and steep escarpment (Figure 2). The plain covers an area of about 70 km² and is at an altitude of about 780 m asl. In contrast, Simav Mountain, which is a horst structure, located to the south of the plain, reaches an altitude of 1,780 m asl.

The stratigraphic sequence of the formations in the Simav region is given in (Figure 3). Paleozoic metamorphic rocks are located at the base of the rock strata in the region. These rocks form the mountains that border the graben on both sides, and outcrop frequently in these mountains. Also, it is known that under the graben, these rock units are underlain by younger sedimentary rocks. The metamorphic rocks are covered by a layer of lower Mesozoic rocks and Jurassic carbonates that have not been metamorphosed, which also overlay the metamorphites in the Simav horst to the south of the graben as well as in the relatively lower Akdağ horst to the north. These rocks are overlain by volcanic rocks and lake sediments of Miocene age that were deposited in the graben along a NNE-SSW axis or formed in relation to those grabens. These formations appear on the Simav horst to the south of the graben as well as on ridges of the arm to the north of the graben, which has risen to a lower altitude. These are followed by younger formations which precipitated or formed together with the Simav graben or at a later time (Akdeniz and Konak, 1979). These are spread out over the graben interior areas, which have been downthrown significantly compared with the horsts on both sides of the Simav graben. The coarse-grained terrestrial sediments, basaltic lava deposits and thick alluvium have created a layer in the graben that is hundreds of meters thick (Öngür, 2004). Based on the existing wells drilled in the region, the fractured reservoir rocks producing hot fluids in the field largely consist of Naşa Basalt, Simav metamorphics and Mesozoic limestones, while the cap rock consists of Tertiary strata of volcano-sedimentary rock. In extensional tectonic regimes like the Basin and Range province and the Anatolia Belt of western Turkey, extensional detachments have created favorable structures for geothermal occurrences. Three

crustal segments, namely central core, southern and northern sub-massifs, differing in structure and cooling history have been identified in Menderes Massif of western Turkey by Ring et al. (2003). The Simav detachment, formed later, reactivated the Eocene Cyclades-Menderes thrust and its initial movement was synchronous with the intrusion of Eğrigöz granites (Ring et al., 2003). After Miocene, western Anatolia underwent the extensional regime that helped build the actual form. This process produced the Simav graben, which has an asymmetric structure. The southern part of the graben is limited by the Simav fault, which is roughly extended in west-east direction for more than 80 km and separates Simav Mountain from Simav plain.
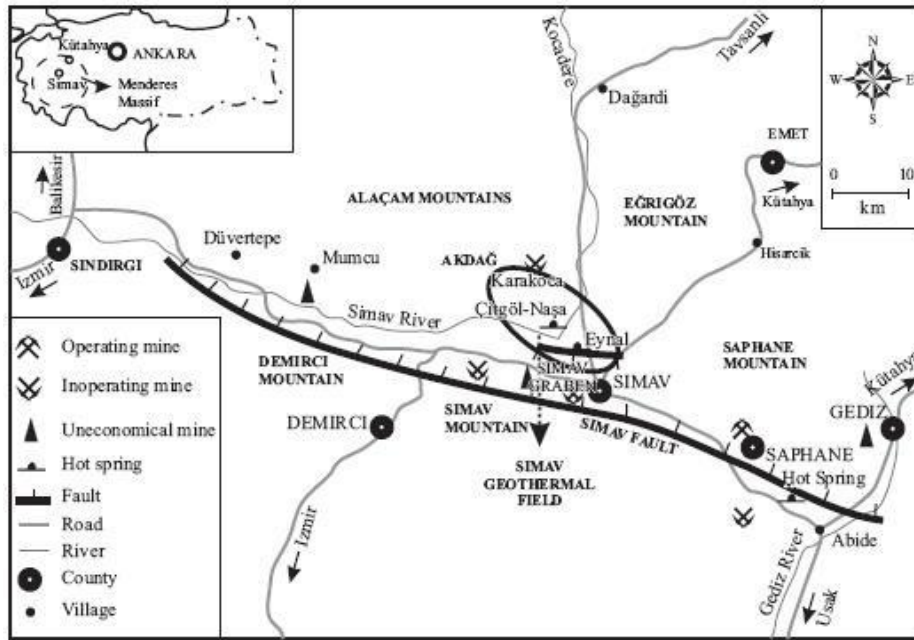

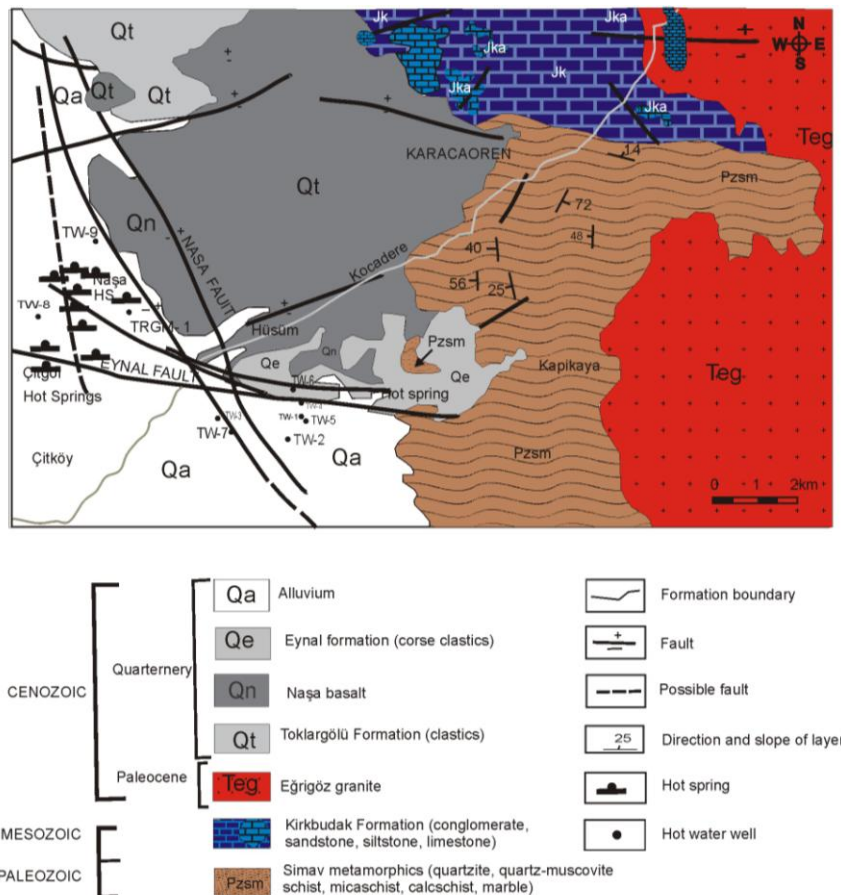**Figure 2: Location map of the study area (Öygür and Erler, 2000).**

Figure 3: Geological map of the study area (Akkuş et al., 2005).

3. MATERIALS AND METHODS

The thermal waters were collected from drilled wells with only one from hotspring. Locations of the sampling points (TW) are shown in Figure 3. Based on the conducted field studies, a total of 10 samples were collected for each analysis (Cation and Anion). In-situ and hydrogeochemical analysis were carried out on these samples. The in-situ analyses such as Temperature, Hydrogen ion concentration (pH), Electrical Conductivity (EC), Total dissolved oxygen (O_2), redox potential (Eh) and alkalinity were conducted on the field. The hydrogeochemical analysis was done at Galtek Chemical Industrial and Trading Ltd., Istanbul, Suleyman Demirel University, Department of Environmental Engineering and Metrohm (34330, Levent-Istanbul). The results are presented in Table 2.

4. HYDROGEOLOGY OF THE LITHOLOGY UNITS

Joints and faults resulting from neotectonic activity caused the developments of secondary porosity and high permeability in limestone and marble. In the study area, three (3) reservoir rocks were determined (Figure 4).

I. Reservoir rocks: The Nasa basalt pinching out in quaternary unit is the shallow reservoir rock. The Nasa basalt and the Toklargölü formation cover an area of 84 km^2 in the study area. The Nasa basalt covered by alluvium and Eynal formation, geothermal fluid production is active in C-1, C-2 (abandoned C-3, C-4, C-5) and N-1, N-2 wells. In addition, hot water has been produced from the first reservoir rocks in some of the other boreholes. The highest temperatures in first reservoir rock were measured at 85m of depth in C-1 well to be 105^0C (Bayram and Şimşek, 2005).

II. Reservoir rocks: The Budagan limestone and the Arıkaya formation having secondary porosity and permeability are the second reservoir rocks. These formations crop out in an area of 25 km^2. These formations have longer lateral extension and are located deeper than first reservoir rocks. Therefore higher temperatures were obtained. Hot waters from EJ-1, EJ-2, E-2, E-3, E-4, E-5, E-6, E-7, E-8, and E-9 are drawn from this reservoir. The highest temperature of 162.47 °C was measured from EJ-1 well (Bayram and Şimşek, 2005).

III. Reservoir rocks: It is possible to consider the presence of third reservoir rock depending on the interbedding of cover and reservoir rocks. The Balıkbası formation crops out in an area of 6 km^2 in the study area. It comprises of secondary porous and permeable marble and underlines the Sarıcasu formation having cover rock characteristics. EJ-1 and EJ-2 wells yield hot water at this reservoir (Bayram and Şimşek, 2005). In the study area, three sealing cap rocks having impermeable characteristics were determined.

I. Cap rocks: The Eynal formation over the Nasa basalt contains impermeable clayey level in places. In wells around the Nasa and Citgöl thermal springs, after alluvium, impermeable levels of formations were cut. This shows that it has characteristics of cap rock. It crops out in an area of 2 km^2 in the study area.

II. Cap rocks: The Akdag volcanic rocks, the Civanadag tuffs and the Kızılbük formation form a thick cap rock. All these units cover an area of 140 km^2 in the study area. The temperature is raised to 162 °C due to the presence of these cap rocks. Meanwhile, a temperature of 105 °C was measured in the reservoir under the first cap rock.

III. Cap rock: The Sarıcasu formation has lateral and vertical transition with the third reservoir rocks. It crops out in an area of 19 km^2 in the study area.

5. HYDROGEOCHEMISTRY

To understand the hydrogeochemical characteristics of the study area, 10 water samples were taken from different geothermal wells across the area representing the total area. Out of these 10 samples, one was collected from a hot spring while the remaining samples were taken from drilled geothermal wells. The in-situ parameters measured are Temperature, pH, Redox potential (Eh), Dissolved Oxygen (O_2), Electrical conductivity (EC), and alkalinity. In summary, the temperature ranges from 61.6 - 91 ^0C, pH is between 7.40 and 8.78 and electrical conductivity ranges from 1620 - 2990 μS/cm. The detailed results are given in Table 1.

The following cations and elements, Na^+, Ca^{2+}, Mg^{2+}, K^+, Pb, SiO_2, Zn, Al, Cr, Cu and As were analyzed using ICP-OES and ICP-MS, while the following anions, F^-, Br^-, Cl^-, SO_4^{2-}, NO_3^-, NO_2^- and PO_4^- were analyzed using Ion-chromatography. The HCO_3^- and CO_3^{2-} were calculated from the alkalinity measurements on the field. For the examination and geochemical analysis of the results, Aquachem v.3.7 (Waterloo Hydr., 1999), Liquid analysis geochemical plotting spreadsheet (Powell and Cumming, 2010), and Solveq (Reed and Spycher, 2001) were used to evaluate the hydrogeochemical characteristics of the study area. The hydrogeochemical analyses are presented in Table 2.
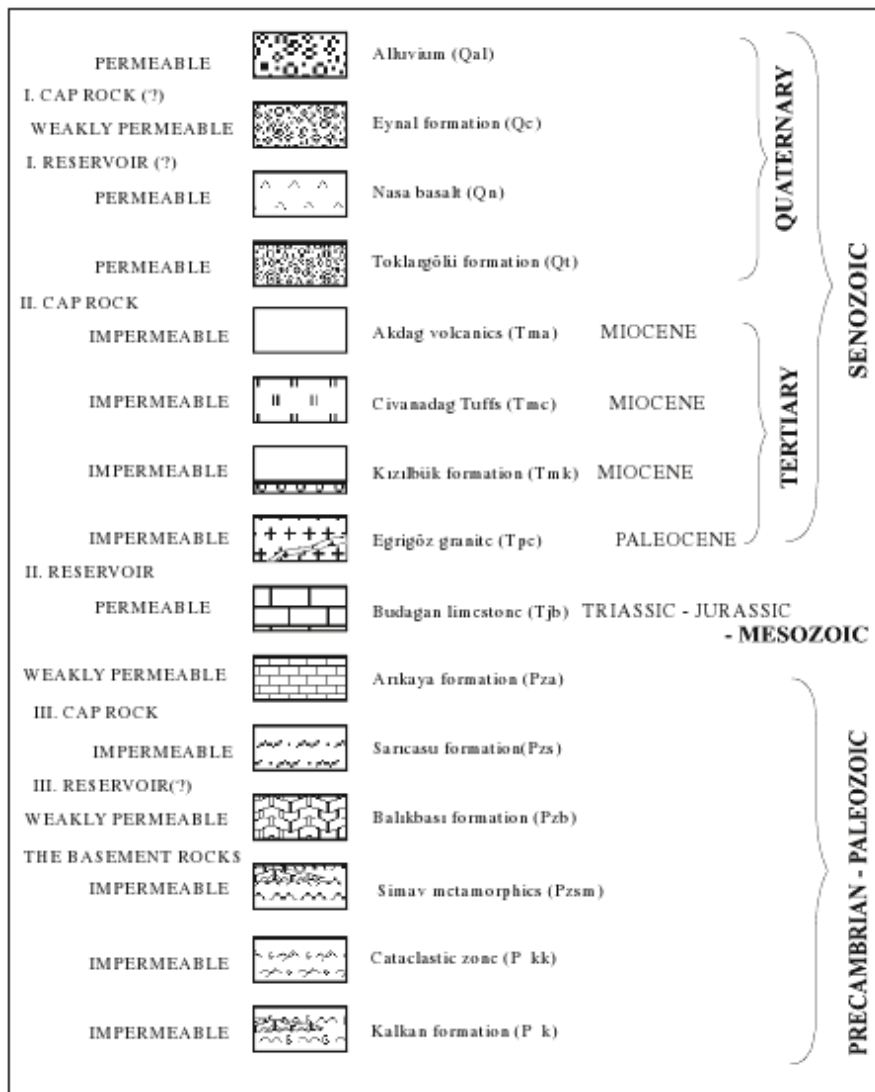
Figure 4: Hydrogeological Characteristics of the rock units (Bayram and Şimşek, 2005).

5.1 Hydrogeochemical Analyses

The results from the hydrogeochemical analyses of the samples from Simav region were evaluated using AquaChem v.3.7 (Waterloo Hydro., 1999) and Liquid analysis spreadsheet (Powell and Cumming, 2010). Diagrams such as piper, schoeller and ternary were prepared to graphically illustrate the hydrochemistry of the water samples and to determine the type of water present in the geothermal system of Simav and environs. According to piper diagram in figure 5, the thermal waters in Simav region can be classified as Na-HCO_3-SO_4 type water while sample TW-10 from Ilicasu kaplicalari is classified as a Na-Ca-SO_4-HCO_3.

Using schoeller diagram (figure 6), the waters from the Simav region can be classified as Na+K > Ca > Mg according to the dominant cations and as HCO_3 > SO_4 > Cl according to the dominant anions.

The Cl-SO_4-HCO_3 ternary diagram is used to classify geothermal fluids on the basis of the major anion concentrations (Giggenbach, 1988). It helps to discern immature unstable waters and gives an initial indication of mixing relationships or geographic groupings. The Cl-SO_4-HCO_3 plot of the samples from the study area shows that the waters plot on the peripheral water region (Figure 7) and it is a bicarbonate water due to the predominant plots on the bicarbonate vertex of the ternary diagram. It shows that the water is more likely related to groundwater heated by steam from deeper reservoir. Hence, it may not give the best predictive result of the reservoir temperature using geothermometer.

The Na+K-Mg-Ca ternary diagram (Figure 8) of the study area shows that the cation is predominantly Na+K as the plots converge at the Na+K corner. This is expected because Na^+ contents of water increase with temperatures while Ca^{2+} and Mg^{2+} contents decrease. Hence the low values of Ca^{2+} and Mg^{2+} in the geothermal waters of the study area. However, sample TW-10 has a high

S/NO	Sample ID	Location	Temp (°C)	pH	Eh (mV)	Dissolved O$_2$	EC (µS/cm)	Alkalinity
1	TW1 (E9)	Eynal	84	8.77	253.4	1.9	2110	10.07
2	TW2 (E10)		90.2	8.72	269.24	7.8	2080	10.07
3	TW3 (EJ1)		70.1	8.44	281.5	2.2	2360	10.40
4	TW4 (E6)		70.2	8.57	298.4	2.8	2410	13
5	TW5 (E8)		91	8.56	328	2.3	2320	13.5
6	TW6 (EJ5)		72	8.78	240	3.1	1903	11.8
7	TW7 (EJ3)		76.1	8.61	281	2.3	2110	13.4
8	TW8	çitgöl	63.7	7.77	50	3.5	1620	9.5
9	TW9	Naşa	61.6	7.86	96.5	3.4	1712	10
10	TW10	Ilicasu	72.5	7.40	115	3.0	2990	16.3

Table 1: In-situ parameters of the thermal waters of Simav and environs.

Ca^{2+} content which is suspected to have moved through a calcite bearing rock. This is true considering the presence of limestone in the area in which the sample was taken.

5.2 Saturation Index

The saturation indices of some carbonates (commonly calcite, aragonite and dolomite; minority siderite and magnesite), Sulphate (commonly gypsum and anhydrite) and silica (commonly quartz and chalcedony) minerals help us to estimate which one of these minerals may precipitate during the extraction and use of the geothermal fluids. These calculations are useful in predicting the presence of reactive minerals and estimating mineral reactivity in a groundwater system (Deutsch, 1997; Gemici and Tarcan, 2002). Saturation indices also help us to evaluate the chemical equilibrium between fluid and rock in a geothermal system. This is accomplished by gathering information about the solubility of minerals in rocks that have undergone hydrothermal alteration and about the activity of the mineral type in the solution. Because of the large number of ions, ion-pairs and complexes in the solution, generating the saturation index for each type as well as activities requires the use of a software program. For this exercise, Solveq (Reed and Spycher, 2001) was used to compute the saturation index. The saturation indices of the thermal waters were calculated at the discharge temperature as well as simulation with increase temperature and measured pH values. Quartz, aragonite, calcite and chalcedony are oversaturated at discharge temperatures while at a recomputed temperature according to the reservoir composition, only quartz, dolomite and chalcedony are oversaturated. According to this saturation indices, scaling of carbonate minerals is expected for the geothermal waters and this coincides with field observation as waters from deep wells cause scaling during extraction. Inhibitors are employed in the prevention of scaling in the drill holes.

5.3 Geothermometer Results of the Thermal Waters

The hydrogeochemical results of the geothermal waters from the study area were evaluated using both silica and cation geothermometers in order to understand the reservoir temperature of the geothermal field. The results of the geothermometers are given in Table 4.

The quartz (conductive and adiabatic) geothermometers for Eynal area (TW1-TW7) calculated the reservoir temperature to be between 191 – 231 °C while Çitgöl (TW8), Naşa (TW9), and Ilicasu kaplıcaları (TW10) are 163 -174 °C, 156 -166 °C and 203 -225 °C respectively. For α-cristobalite, β-cristobalite and amorphous silica, proposed by Fournier (1977), in Eynal region, the reservoir temperatures gave values between 83 –182 °C and Çitgöl, Naşa, with Ilicasu kaplıcaları gave between 50 - 124 °C, 43 – 115 °C and

Sample ID	Temp (^{0}C)	pH	Eh (mV)	EC (μS/cm)	O_2 mg/l	Ca	K	Mg	Na	F	Cl	Br	NO_3	NO_2	PO_4	SO_4	HCO_3	CO_3	SiO_2	Cr	Al	Zn	Pb	Cu	As
TW1	84,0	8,77	-253,4	2110	1,9	12,3	63,7	2,8	445,5	19,91	65,9	2,44	30,56	0	32,4	401,27	414,8	108	295	0,003	0,19	0,01	0,002	0,005	0,48
TW2	90,2	8,72	-269,24	2080	7,8	13,7	63,7	2,6	633,5	19,6	64,49	2,44	31,55	0	0	402,67	427	90	382,3	0,003	0,22	0,03	0,004	0,02	0,43
TW3	70,1	8,44	-281,5	2360	2,2	14,2	54,2	2,5	509,2	14,75	71,82	2,47	30,52	0	0	419,51	683,2	54	367,3	0,003	0,24	Nd	Nd	0,002	0,5
TW4	70,2	8,57	-298,4	2410	2,8	12,8	50,1	2,5	506,5	17	71,41	2,47	30,55	0	0	423,45	640,5	60	332,7	0,005	0,22	0,13	0,001	0,01	0,6
TW5	91,0	8,56	-328,0	2320	2,3	14	52,5	2,4	509,2	15,76	70,71	2,44	30,53	0	0	415,81	610	90	325,4	0,006	0,18	Nd	Nd	0,002	0,46
TW6	72,0	8,78	-240,0	1903	3,1	28,6	62	3,9	567,2	11,45	49,71	0	0	0	0	323,12	469,7	108	349,6	0,005	0,12	0,06	0,002	0,005	0,43
TW7	76,1	8,61	-281,0	2110	2,3	24,6	60,3	3,6	545	12,71	58,86	0	0	0	0	364,85	573,4	78	332,1	0,003	0,002	Nd	Nd	0,002	0,31
TW8	63,7	7,77	50	1620	3,5	26	29,6	5	328	6,3	43,64	0	0	2,84	0	299,21	579,5	bdl	181,9	0,003	0,005	Nd	Nd	0,002	0,24
TW9	61,6	7,86	96,5	1712	3,4	68,2	29,6	11,8	302	3,49	48,64	0	0	3,08	0	344,08	610	bdl	160,2	0,008	0,008	Nd	Nd	0,002	0,3
TW10	72,5	7,40	115,0	2990	3,0	209	69,7	74,1	548,2	2,21	83,53	2,48	0	0	0	827,21	994,3	bdl	355	0,002	Nd	Nd	Nd	0,004	0,09

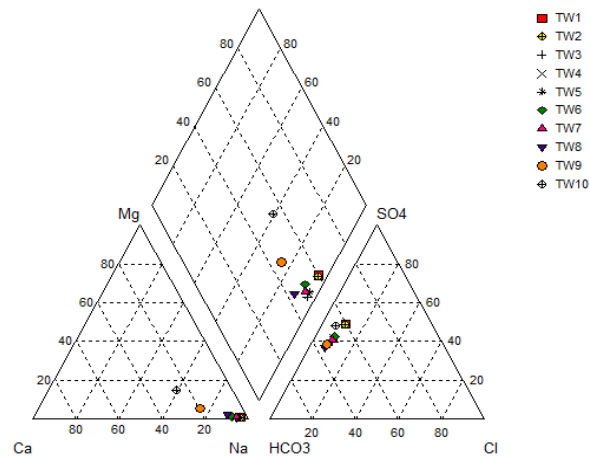**Table 2: Results of the hydrogeochemical analysis of thermal waters in the study area.**

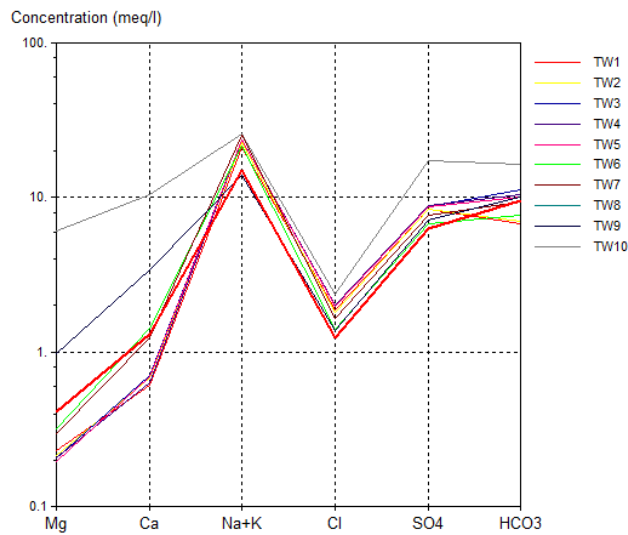**Figure 5: Piper diagram of thermal waters from the study area**

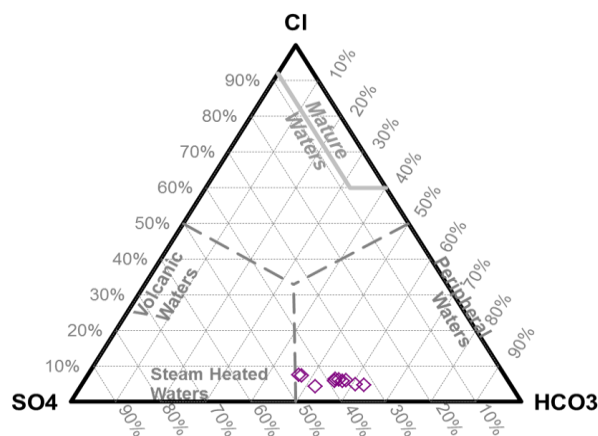**Figure 6: Schoeller diagram of the thermal waters in the study area**

Figure 7: Cl-SO₄-HCO₃ ternary diagram showing that the waters are immature.

98-175 ^{0}C respectively. The Na-K-Ca-Mg correction cation geothermometer gave reservoir temperatures close to the measured reservoir temperature on site in Eynal. The calculated temperature for Eynal is between 148-163^{0}C. The other cation geothermometers gave values that are too high (Table 4).

The Na-K-Mg$^{1/2}$ ternary diagram was proposed by Giggenbach (1988) as a method to make a clear distinction between the thermal waters that are suitable for the estimation of reservoir temperature by the application of solute geothermometers. The waters from

Sımav geothermal field fall in the immature waters (figure 9). Waters from Eynal (TW1-TW7) are located close to the boundary of partially equilibrated waters. The other three samples (TW8-TW10) fall closer to cold groundwaters suggesting that they have mixed with a greater portion than the Eynal thermal waters.
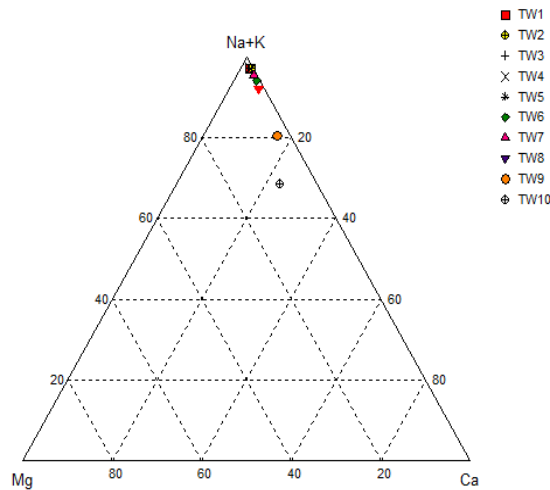

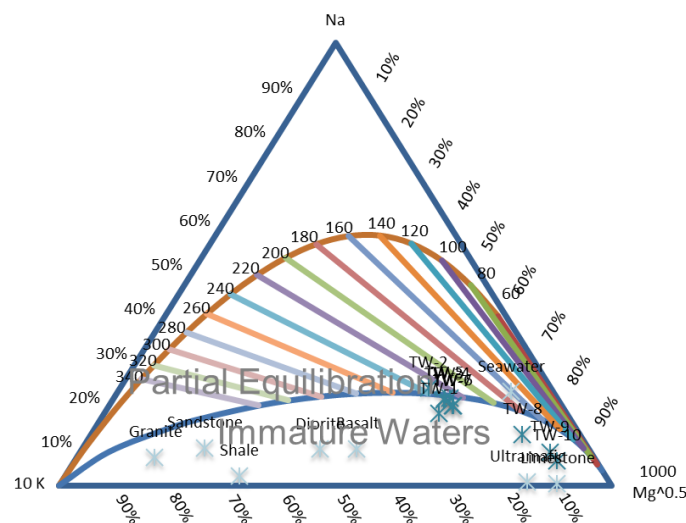**Figure 8: Na+K-Mg-Ca ternary diagram of thermal waters from the study area.**

Figure 9: Distribution of the thermal waters from the study area in the Na-K-Mg$^{1/2}$ ternary diagram.

6. ISOTOPE GEOCHEMICAL FEATURES

The isotope chemistry of a geothermal system provides information about the origin, dating and residence time of the geothermal fluid, the physical processes to which the water is subjected, the fluid-rock interaction and the reservoir.

For this study, the isotopic data from Bayram and Şimşek (2005) were used in assessing the origin of the geothermal waters from the study area (Table 3). The geothermal waters from the study area plot along the meteoric trend line suggesting local meteoric water (Figure 10). Furthermore, they are enriched in δ^{18}O. This situation points to the existence of fluid-interaction in the system and/or boiling due to the high temperature in the reservoir. Also, the change of δD content in the waters may indicate that the system is fed by waters from a high altitude or come from long distance.
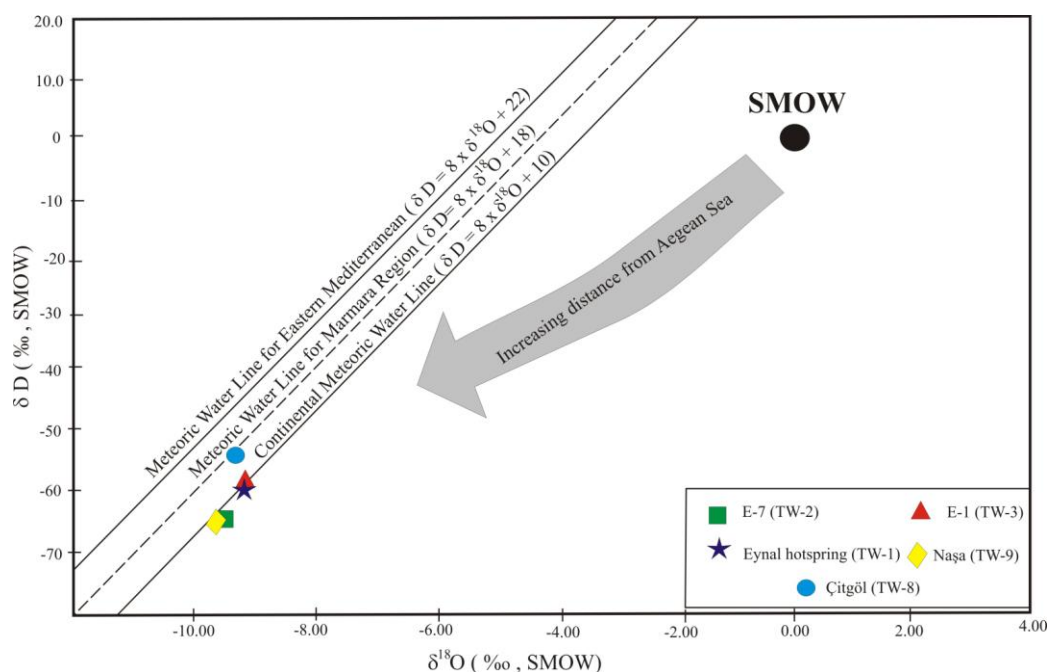
Figure 10: δD vs δ¹⁸O of the Simav thermal waters.

Sample ID	$\delta^{18}O.$	δD	δ^3H
E-7 (TW-2)	-9.34	-65.3	0.78
Eynal hotspring	-8.94	-62.1	0.83
E-1 (TW-3)	-9.08	-60.1	0.36
Çitgöl (TW-8)	-9.23	-55.9	0.64
Naşa (TW-9)	-9.62	-66.7	1.44

Table 3: Isotope analysis results.

7. HYDROGEOLOGICAL MODELING OF SIMAV GEOTHERMAL SYSTEM

Several hot springs, ranging in temperature from 61.6 to 91 ^{0}C, emanate from alluvium along the northern margin of the basin, where sediments are juxtaposed against Naşa basalt along a complex, anastomosing part of the S-dipping antithetic fault system. Several of these faults are marked by Quaternary fault scarps. The main E-W trending line of hot springs in the Eynal area is situated in the hanging wall of this anastomosing normal fault system. There is reason to believe that there exists a high-temperature system (>180 ^{0}C) at depth because of the discovery of opaline sinter at the surface along some of the hot springs. Existing wells penetrate to 958 m, but the main reservoir may not be discovered yet. This reservoir may lie in the metamorphic basement and partly in the Miocene igneous rocks (Faulds et. al., 2010).

The geothermal activity at Eynal may be primarily controlled by multiple fault intersections within the anastomosing S-dipping normal fault system, whereby highly fractured steeply dipping conduits have provided pathways for fluid circulation. At depth, the waters react with heated rocks. The CO_2, SO_2, HCl and H_2S that escaped from the magma reached the geothermal water reservoir where equilibrium is reached between altered rocks and fluids. Thus the thermal waters escape into tectonic zone of weakness, namely the Simav fault, as hot springs to the surface (Figure 11).

Sample Name	Amorphous Silica	Alpha Cristobalite	Beta Cristobalite	Chalcedony conductive	Quartz conductive	Quartz adiabatic	Na-K-Ca	Na-K-Ca Mg corr	Na/K Fournier 1979	Na/K Truesdell 1976	Na/K Giggenbach 1988	Na/K Tonani 1980	Na/K Nieva & Nieva 1987	Na/K Arnorsson 1983	K/Mg Giggenbach 1986
TW-1	83	160	110	192	209	191	226	163	250	230	263	270	236	235	136
TW-2	104	182	132	217	231	207	210	161	217	188	233	224	204	196	137
TW-3	101	178	128	213	227	205	209	157	222	194	237	231	209	201	132
TW-4	93	170	120	203	219	198	205	150	216	186	231	222	203	194	130
TW-5	91	168	118	201	217	197	207	156	220	191	235	227	206	198	132
TW-6	97	174	124	208	223	202	200	148	225	197	240	234	211	204	129
TW-7	93	170	120	203	219	198	204	149	226	199	241	235	212	206	130
TW-8	50	124	74	152	174	163	155	97	208	177	224	211	195	185	104
TW-9	43	115	66	142	166	156	125	87	215	185	231	221	202	193	92
TW-10	98	175	125	209	225	203	138	47	238	215	252	254	225	221	90

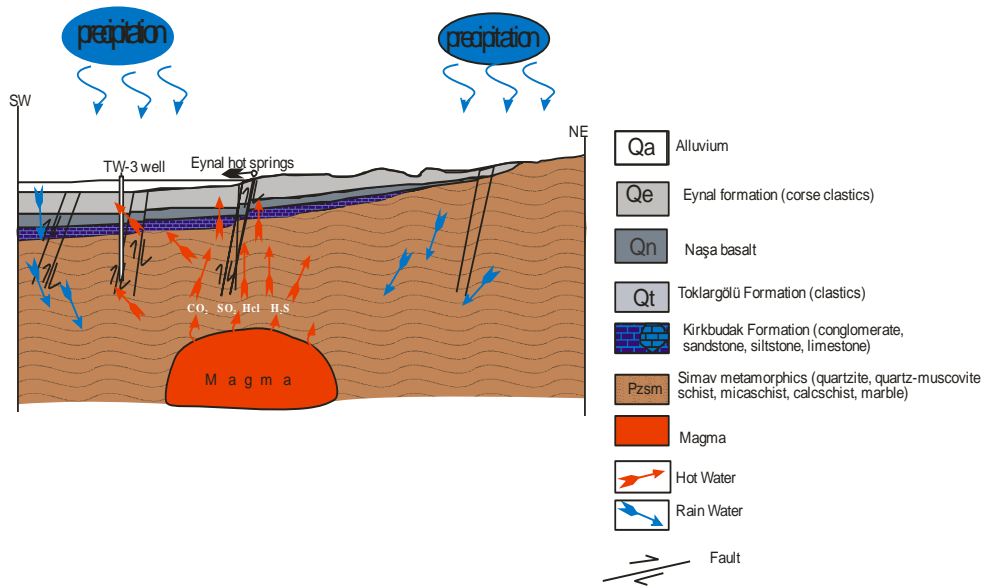**Table 4. Solute geothermometer results of the thermal waters from the study area.**

Figure 11: A simplified model of Simav geothermal system.

7.1 Relationship between Tectonics and Heat Source of Simav Geothermal System

Turkey is known to have many low to moderate temperature geothermal resources (Serpen and Mihcakan, 1999; Palabiyik and Serpen, 2008) and most of these resources are related to important fracture systems. The major geothermal systems of western Turkey are all structurally similar geothermal occurrences. A localized extensional tectonic regime prevails in western Anatolia where the lithospheric stresses are mostly related to the continental collision of Alpine-Himalayan zone. Western Anatolia is characterized by east-west trending mountain range, and deep sediment filled valleys. The region experienced a north-south shortening until the beginning of the late Miocene. At the beginning of the Tortonian, the region experienced an extension, and the partially melted crust began stretching to form a thin and a brittle crust (Yılmaz, 1989; Alptekin et al., 1990; Gemici and Tarcan, 2002). There are a few E-W trending grabens in Western Turkey. Most of the important geothermal areas of Turkey are located in the rims of these grabens. Simav graben is one of them and formed by WNW-ESE trending and north-dipping fault. The Simav graben is a Pliocene–Quaternary structure with a distinct topographical depression, extending for about 150 km. The graben cuts the NE–SW trending Demirci, Selendi and Akdere basins and is regarded as one of the latest products of N–S extensional tectonics, in contrast to the Aegean grabens that began to develop during late Oligocene–Early Miocene times (Seyitoğlu, 1997). The southern side of the Simav half-graben cut the Neogene basins and also the Simav detachment fault. Bozkurt et al. (2011) suggested an episodic Simav detachment fault activity between ca. 30 and 8Ma. The occurrence of volcanic rocks intercalated with sediments in graben-type structures, and extensional uplifting of the region shows that (Early to Middle Miocene) magmatism in Simav region took place under an extensional tectonic regime in a back-arc position.

The graben is bounded on the south by a major N-dipping normal fault that has accommodated several kilometers of normal slip and is referred to as the Simav fault. This fault is part of a large semi-continuous WNW to EW striking fault zone that extends across much of western Turkey and may have accommodated some strike-slip displacement. A system of S-dipping antithetic normal faults with much less displacement bounds the normal margin of the basin (Faulds et. al., 2010). The Simav fault penetrates very deep to communicate a deep heat sweep of naturally convecting meteoric waters in the metamorphic crust. Hochstein et al. (1990) pointed out that fracture zone systems, which are driven by higher than normal heat flow; occur in areas underlain by thinner continental type of crust (*i.e.*, systems in the Basin and Range tectonic province of USA and Menderes Massif of Turkey). An earlier theoretical study by Kassoy and Zebib (1978) also showed that fluid convection can occur in a narrow fracture zone which stands in a crustal environment with normal temperature. The Simav geothermal system is thought to be controlled by the active Simav fault and probably driven by higher than normal heat flow, 110mW/m2 (Ilkisik, 1995; Palabiyik and Serpen, 2008), in the Aegean region of Turkey, and terrain-induced forced convection. With prevailing temperatures of about 160 ºC at economic depths (less than 1 km) within the fracture zone reservoir, the Simav geothermal system resembles "the fracture zone systems with high temperatures at sweep base" described by Hochstein (1990).

Bello et al.

8. CONCLUSION

Joints and faults resulting from neotectonic activity in the study area caused the developments of secondary porosity and high permeability in limestone and marble. Four reservoir rocks are determined in the study area. The reservoir rocks are Naşa basalt, Budağan limestone, Arıkaya formation and Balıkbası formation, all hosting the geothermal waters in the study area. Three cap rocks were also identified in the study area and they are the Eynal formation, Akdağ and the Sarıcasu formation.

The geothermal waters have surface temperatures between 61.6 and 91 ºC and are mostly Na-HCO_3-SO_4 type water while sample TW-10 from Ilicasu kaplicalari is classified as a Na-Ca-SO_4-HCO_3. They can also be classified as Na+K>Ca>Mg according to the dominant cations and as HCO_3>SO_4>Cl according to the dominant anions with Schoeller diagram. The Cl-SO_4-HCO_3 plot of the samples from the study area shows that the waters plot on the peripheral water region and it is a bicarbonate water due to the predominant plots on the bicarbonate vertex of the ternary diagram. It shows that the water is more likely related to groundwater heated by steam from deeper reservoir. Hence, it may not give the best predictive result of the reservoir temperature using geothermometer.

The geothermal waters from the study area plot along the meteoric trend line suggesting local meteoric water. Furthermore, they are enriched in ^{18}O. This situation points to the existence of fluid-interaction in the system and/or boiling due to the high temperature in the reservoir. Also, the change of deuterium content in the waters may indicate that the system is fed by waters from a high altitude or come from long distance.

REFERENCES

Akdeniz, N and Konak, N.: Simav-Emet-Tavşanlı-Dursunbey-Demirci yörelerinin jeolojisi –(Geology of Simav –Emet-Tavşanlı-Dursunbey-Demirci area)- *MTA report,* **6547** (1979).

Akkuş I., Akilli H., Ceyhan S., Dilemre A., Tekin Z.: Turkey's Geothermal Resource Inventory (in Turkish), *Mineral Research and Exploration of Turkey (MTA),* Inventory series **201** (2005) 521p.

Alptekin, Ö., Ezen, U., Uçer, S.B.: Heat flow, seismicity and the crustal structure of Western Anatolia. *Proceedings*, International Earth Sciences Congression Aegean Regions, Vol-II, (1990), İzmir, Turkey.

Bayram Ferhat A. and Şimşek Sakir.: Hydrogeochemical and Isotopic Survey of Kütahya-Simav geothermal field. *Procdings,* World Geothermal Congress (2005), Antalya, Turkey.

Bozkurt E., Satır, M., Buğdaycıoğlu, Ç.: Surprisingly young Rb/Sr ages from the Simav extensional detachment fault zone, northern Menderes Massif, Turkey. *Journal of geodynamics* **52**, (2011) 406-431.

Deutsch, W.J.: Groundwater Geochemistry: Fundamentals and Applications to Contamination. (1997) Lewis, USA.

Faulds, J., Coolbaugh, M., Bouchot, V., Moeck, I., Oğuz, K.: Characterizing structural controls of geothermal reservoirs in the Great Basin, USA and western Turkey: Developing successful exploration strategies in extended terranes. *Proceedings*, World Geothermal Congress, Bali Indonesia, 2010.

Gemici Ünsal and Tarcan Gültekin.: Hydrogeochemistry of the Simav geothermal field, Western Anatolia, Turkey. *Elsevier Journal of Volcanology and geothermal research* **116** (2002) 215-233.

Giggenbach, W.F.: Geothermal solute equilibria. Derivation of Na-K-Mg-Ca geo-indicators. *Geochim Cosmochim Acta*, **52**, (1988) 2749-2765.

Hochstein, M.P.: Geothermal resources, classification and assessment of geothermal resources: Pisa, Italy, International Institute for Geothermal Research, *International school of geothermics*, **2**; (1990) 31-57.

Hochstein, M.P., Zhongke, Y., Ehara, S.: The Fuzhou geothermal system (People's Republic of China): Modelling study of a low temperature fracture-zone system: *Geothermics*, **19** (1), (1990) 43-60.

Ilkisik, M.: Regional heat flow in Western Anatolia using silica temperature estimates from thermal springs: *Tectonophysics*, **244**, (1995) 175-184.

Kassoy, D.R., Zebib, A.: Convection fluid Dynamics in a model of a fault zone in the earth crust: *Journal of fluid mechanics*, **88,** (1978) 769-792.

Konak, N.: Simav surrounding geology and the evolution of its metamorphic rocks. *İstanbul Geosci.* 313-337 (1982).

Nicholson Keith.: Geothermal fluids, Chemistry and Exploration Techniques, *Springer-Verlag* Berlin Heidelberg, Germany (1993)**.**

Ongur, T.: Simav jeotermal alanının kapasitesi. Jeoloji değerlendirmesi, *Ege Enerji A.Ş.*, unpublished, İstanbul (2004).

Oygür Vedat and Erler Ayhan.: Simav Grabeninin metalojenisi (İç-batı Anadolu, Türkiye) (metallogeny of the Simav graben (Inner-Western Anatolia, Turkey) *Türkiye Jeoloji Bülteni cilt.* **43**, no.1, (2000) 7-19.

Bello et al.

Palabıyık Yıldıray and Serpen Umran.: Geochemical assessment of Simav geothermal field, Turkey. *Revista mexicana de Ciencias Geologicas,* **V.25**, num 3, (2008) P.408-425.

Powell, Tom and Cumming William.: Spreadsheet for geothermal waters and gas geochemistry, *Proceedings* 35th workshop on geothermal reservoir engineering, Stanford University, California (2010). SGP-TR-188.

Reed M. H. and Spycher N. F.: User guide for SOLVEQ, a program for computing aqueous and mineral and gas equilibrium, *Department of geological sciences*, University of Oregon (2001).

Ring, U., Johnson, C., Hetzel, R., Gessner, K.: Tectonic denudation of a late Cretaceous-Tertiary collisional belt: Regionally symmetric cooling patterns and their relation to extensional faults in Anatolide belt of Western Turkey: *Geological Magazine*, **140** (4), (2003) 421-441.

Saroğlu, F., Boray, A., and Emre, O.: Active faults of Turkey, *Mineral Res. Explor. Inst.* Turkey, unpubl. **Report 8643**, (1987) . 394pp.

Saroğlu, F., Emre, O., and Kuscu, I.: 1:1000000 Active fault map of Turkey, *MTA* (1992).

Serpen, U., Mihcakan, M.: Heat flow and related geothermal potentials of Turkey. Geothermal Resources Council (GRC) Annual Meeting. *GRC transactions*, **23**, (1999) 485-490.

Seyitoğlu Gürol.: The Simav Graben, An example of young E-W trending structures in the late Cenozoic extensional system of western Turkey. *Tr J. of Earth Sciences* **6** (1997) 135-141 (TÜBİTAK).

Şengor, A.M.C., Goru, N., and Varoğlu, F.: Strike-Slip faulting and related basin formation in zones of tectonic escape; Turkey as a case study, strike-slip deformation, Basin formation and sedimentation, *Society of Economic paleontologists and mineralogists* special publication, **37** (1985).

Waterloo Hydrogeologic, AquaChem v.3.7: Aqueous geochemical analyses, plotting and modelling, (1999) 184 p.

Yılmaz, Y.: An approach to the Origin of Young Volcanic rocks of Western Turkey. In: Tectonic evaluation of Tethyan Regions *Kluwer Academic Publishers, Dordrecht*. (1989), p159-189.

Yılmaz, Y.: When did the Western Anatolia Grabens begin to develop? In: Tectonics and magmatism in Turkey and the surrounding area. *Geological Society London Special Publications*, **173**, (2000) 333-384.